Journal of Materials Chemistry A

Accepted Manuscript

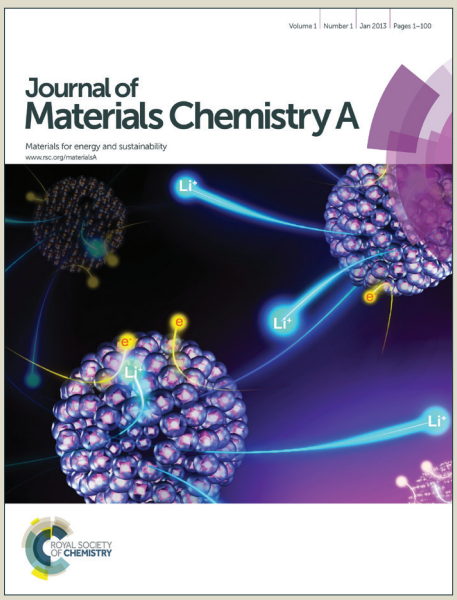

ROYAL SOCIETY OF CHEMISTRY

www.rsc.org/materialsA

Journal of Materials Chemistry A

ARTICLE

Influence of anionic surface modifier on thermal stability and mechanical properties of layered double hydroxide/polypropylene nanocomposites

Received 00th January 20xx,
Accepted 00th January 20xx

DOI: 10.1039/x0xx00000x

www.rsc.org/

Jae-Hun Yang, [a,‡] Wei Zhang,[a,‡] Hyunju Ryu,[a] Ji-Hee Lee,[a] Dae-Hwan Park,[a] J. Yoon Choi,[b] Ajayan Vinu,[c] Ahmed A. Elzatahry[d,e] and Jin-Ho Choy [a,*]

Organo-layered double hydroxide/polypropylene (LDH/PP) nanocomposites were successfully synthesized via solution blending method. As an attempt to improve the compatibility with hydrophobic PP, the LDH surface was modified by the incorporation of various anionic surfactants via electrostatic interaction with LDH cationic layers. Surfactants were selected by considering aliphatic carbon chain length (laurate, palmitate, stearate and dodecylsulfate) and anionic functional groups ($-COO^-$, $-OPO_3^{2-}$, $-OSO_3^-$) with the purpose of optimizing the homogeneous dispersion in PP matrix. In PP nanocomposites containing LDH modified with alkyl carboxylate, the (*00l*) X-ray diffraction (XRD) peaks originating from organo-LDH were not observed, indicating that organo-LDH layers were fully exfoliated and homogeneously dispersed within PP matrix, which were also confirmed by cross-section TEM analysis. However, PP nanocomposites containing LDH modified with dodecyl sulfate and lauryl phosphate showed broad (*00l*) XRD peaks, indicating that organo-LDH was partially exfoliated. According to the thermogravimetric analysis, the thermal stability ($T_{0.5}$) of organo-LDH/PP nanocomposites were significantly improved by 37 K- 60 K, depending on the type and loading content of organo-LDH compared to pristine PP. PP nanocomposites containing well-dispersed organo-LDH showed substantial enhancement of elastic modulus with little decrease of tensile strength. These results are due to the increased interface volume fraction provided by the exfoliated LDH nanosheets.

Introduction

Polymer nanocomposites with various inorganic nonofillers such as layered silicates,[1-5] carbon nanotubes,[6-7] polyhedral oligomeric silsesquioxanes,[8-9] for enhancing corrosion resistance, gas barrier property, thermal stability, mechanical strength and flame retardation have been reported substantially. Those improvements were primarily due to the homogenous dispersion of inorganic nanofillers within polymer matrix and the increased interaction strength between the polymer segments and inorganic nanofillers. High aspect ratio and large surface area of inorganic nanofiller could result in highly improved properties, such as thermal stability and mechanical strength, due to a high volume fraction of an interface area between the polymer matrix and the nanoparticles.[5] Since Toyota researchers reported a nylon 6-clay nanocomposite with the improved physical properties in 1993,[10] much of academic interest has been focused toward polymer nanocomposites with layered silicates due to their natural abundance along with good mechanical strength enhancer. On the contrary, LDH, which has been relatively less focused, with two dimensional structure similar to layered silicates could be a promising inorganic nanofiller via a soft-chemical process to produce the LDH nanosheets with high aspect ratio.[1,11]

LDHs, also known as hydrotalcite-like materials and anionic clays, have a general formula of $[M^{2+}_{1-x}M^{3+}_x(OH)_2]^{x+}(A^{m-})_{x/m}{\cdot}nH_2O$, where M^{2+} is divalent metal cation such as Mg^{2+}, Zn^{2+}, Fe^{2+}, Ni^{2+}, etc. and M^{3+} is trivalent metal cation such as Al^{3+}, Cr^{3+}, Fe^{3+}, Ga^{3+}, etc. and A^{m-} is interlayer anion such as CO_3^{2-}, NO_3^-, Cl^-, and other anionic species.[1-2] LDH structure is based on brucite-like layers, where Mg^{2+} ion is octahedrally coordinated with 6 hydroxo-ligands to form octahedrons and are bound one another by sharing edges to form infinite two dimensional sheets, and those sheets are stacked to build up lamellar structures via hydrogen bonding. However, divalent metal cations are substituted with trivalent metal cations in the LDH structure, which results in a positive charge on the LDH layer. To neutralize the positive charge of the LDH layer,

[a] Center for Intelligent Nano-Bio Materials (CINBM), Department of Chemistry and Nano Science, Ewha Womans University, Seoul 120-750, Republic of Korea.
[b] Fire & Safety Evaluation Technology Center, Energy & Environment Business Division, Korea Conformity Laboratories, Chungbuk, Republic of Korea.
[c] Australian Institute for Bioengineering and Nanotechnology, The University of Queensland, Brisbane 4073, QLD, Australia.
[d] Materials Science and Technology Program, College of Arts and Sciences, Qatar University, P. O. Box 2713, Doha, Qatar.
[e] Department of Chemistry, Petrochemicals Research Chair, King Saud University 2455 Riyadh 11451, Kingdom of Saudi Arabia.
† Electronic Supplementary Information (ESI) available: See OI: 10.1039/x0xx00000x.
‡ These authors contribute equally to this work.

anionic species are placed in the gallery region of LDHs. Since the type of metal ions and the mixing ratio of divalent to trivalent metal cations in the LDHs are easily tunable and the interlayer anions can be easily exchanged with other anionic species, LDHs are applicable as catalysts,[12] halide scavengers,[13] absorbents,[14] drug delivery carriers,[15] or nanofillers in polymer nanocomposites.[16-21]

LDHs composed of Mg, Zn, and Al are preferred as inorganic fillers within polymer matrix since the usage of these metals preserves the original color of polymers. In general, the property of LDH-polymer nanocomposites are affected by the compatibility and dispersity of LDH in polymer matrix. However, pristine LDH with hydrophilic surface property is not compatible with hydrophobic polymers such as polypropylene (PP) or polystyrene (PS). In order to apply LDHs as an inorganic filler in these polymer nanocomposite, hydrophobic modification of the surface property of LDH is necessary, which can be achieved by intercalating anionic surfactant with hydrophobic aliphatic carbon chain such as fatty acids and dodecylsulfate. Hydrophobic polymer chains can easily access into the interlayer of LDH when the hydrophobic interlayer is swelled, resulting in polymer nanocomposites with highly dispersed LDH. Examples include polymer intercalated LDH nanocomposites or polymer nanocomposites containing exfoliated LDH *via* various methods such as *in situ* polymerization,[17] solution-blending,[18] and melt-blending[19] methods.

Compatibilizers such as maleic-anhydride-grafted polyolefins or organo-LDH with nano-size were reportedly used for improved dispersion of LDH in PP matrix.[18-20] In this study, we report preparation of PP nanocomposites containing LDH without compatibilizers via a solution blending method. For this purpose, LDHs were modified with with various anionic surfactants, such as lauric acid (LA), palmitic acid (PA), stearate (SA), lauryl phosphate (LP), or dodecyl sulfate (DS). Herein, we systemically discuss the physicochemical properties, such as thermal stability and mechanical properties, of prepared PP nanocomposites containing the hydrophobically modified LDHs. appropriate.

Experimental Section

Materials

Magnesium nitrate hexahydrate (>98.0%), magnesium chloride hexahydrate (>98.0%), aluminum nitrate nonahydrate (>98.0%), aluminum chloride hexahydrate (>97.0%), lauric acid (LA, >99.0%), sodium hydroxide (98%), palmitic acid (PA, >95.0%), Xylene (>80%), and methyl alcohol (>99.5%) were purchased from DaeJung Chemical & Metals Co., LTD. Sodium stearate (Na-SA, extra pure) was purchased from Junsei Chemical Co., LTD. Sodium lauryl phosphate (LP, >97.5%) was purchased from Nikko Chemicals. Co., LTD. Sodium n-dodecyl sulfate (DS) was purchased from Kanto Chemical. Co., INC. Polypropylene (PP) was purchased from Lotte Chemical Co., LTD. All the chemicals were used without further purification.

Synthesis of organo-LDHs

The magnesium aluminum LDHs (Mg/Al = 2) modified with anionic surfactants such as LA, PA, SA and DS were prepared by the conventional coprecipitation method. Briefly, the anionic surfactants were dissolved in the mixed solution of water and ethanol (volume ratio1:1) at 65 ^{o}C, and pH of the solution was adjusted to 10.0 (± 0.2) with 1.0 M NaOH aqueous solution. Then, NaOH (1.0 M) solution and the mixed aqueous solution of $Mg(NO_3)_2{\cdot}6H_2O$ (0.2 M) and $Al(NO_3)_3{\cdot}9H_2O$ (0.1 M) were simultaneously and drop-wisely added into the anionic surfactant solution with maintaining pH at 10.0 (± 0.2) at 65 ^{o}C to form the white precipitate. In this reaction, the molar ratio of anionic surfactant to Al was fixed to 1.2. The resulting white precipitate suspensions were further aged for 16h, and then were collected by centrifugation and washed with the mixed solution of water and ethanol (50 vol%, 65 ^{o}C) to completely remove unreacted ions. The washed samples were freeze-dried for 48 hours, and the samples were denoted as LA-LDH, PA-LDH, SA-LDH and DS-LDH, respectively. Since LP-LDH could not be synthesized via coprecipitation method due to the strong complexing power between metal ions and phosphate group of LP, LP-LDH was prepared via ion-exchange reaction. At first, the host LDH, Cl^- intercalated Mg_2Al-LDH (Cl-LDH), was synthesized via the upper condition, but the only differences were that $MgCl_2{\cdot}6H_2O$ (0.2M) and $AlCl_3{\cdot}6H_2O$ (0.1 M) was used instead of $Mg(NO_3)_2{\cdot}6H_2O$ (0.2 M) and $Al(NO_3)_3{\cdot}9H_2O$ (0.1 M), and anionic surfactant and ethanol were not used. Thus prepared Cl-LDH was dispersed in deionized water, and then sodium laurylphosphate aqueous solution was added into that suspension, in which the molar ratio of LP to Al of Cl-LDH was 1.2. The ion-exchange reaction was carried out at 65 ^{o}C for 16 hours under vigorous stirring. After the ion-exchange reaction, the sample (LP-LDH) was completely washed with deionized water to remove unreacted LP, ions such as Na^+ and Cl^-, and then finally freeze-dried for 48 hours. In order to prevent the carbonate contamination in all the samples, the decarbonated water was used throughout the synthesis, and the coprecipitation reaction and ion-exchange reaction were carried out under nitrogen gas flow.

Synthesis of PP/organo-LDH nanocomposites

PP nanocomposites containing five different organo-LDHs (LA-, PA-, SA-, LP- and DS-LDH) were prepared individually by one-step solution blending method. At first, 0.3 g of organo-LDH was dispersed in 40 mL xylene respectively, and the suspension was refluxed at 120 ^{o}C for 24 hours under vigorous stirring, resulting in almost exfoliated organo-LDHs with transparency (†ESI Fig. S1). The prepared organo-LDHs suspension was mixed with 60 mL of PP solution dissolved in xylene (10 g/ 60 mL) at 120 ^{o}C for 24 hours under vigorous stirring. The organo-LDH/PP nanocomposite was separated by solvent extraction method.[18] In brief, the resulting PP xylene solution containing organo-LDH nanosheets was added into 200 mL methanol to give rise to white precipitate. The obtained powders were filtered and dried in vacuum oven at

100 °C to remove the residual xylene (3 phr organo-LDH/PP nanocomposites.[22] In order to investigate the effect of organo-LDH loading content in PP nanocomposites, 1 phr, 6 phr, 9 phr and 12 phr LA-LDH nanocomposites were also prepared through the same preparation process except the used amount of LA-LDH (0.1 g, 0.6 g, 0.9g, 1.2g, respectively) instead of 0.3g of LA-LDH in synthetic process of 3 phr LA-LDH/PP nanocomposite.

Characterization

Powder X-ray diffraction (PXRD) patterns of the prepared samples such as organo-LDHs and the organo-LDH/PP nanocomposites were recorded with Rigaku D/MAX RINT 2200-Ultima+ diffractometer equipped with Ni-filtered Cu-Kα radiation (λ=1.5418 Å) at 40 kV and 30 mA. Fourier transform infrared (FT-IR) spectra were obtained with a JASCO FT/IR-6100 spectrometer by the KBr disk method. Transmission electron microscopoic (TEM) images were obtained using a JEOL JEM-2100F field emission transmission electron microscope. PP nanocomposites samples for TEM analysis were prepared with a RMC CryoUltramicrotome (CRX), in which sectioning was conducted at –120 °C with sample thickness between 60 nm - 80 nm and cutting speed of 0.3 mm/min. The thermal behavior of the prepared samples was analyzed by using a TA Instruments SDT-Q600 thermogravimetric analyzer with air flow rate of 200 mL/min and heating rate of 10 °C/min in the range between 40 °C and 800 °C. For the recrystallization and melting point of PP and PP nanocomposites, differential thermal analysis (DTA) curves were recorded through the following process; all the samples was heated from 50 °C to 220 °C at a rate of 10 °C/min, and cooled to 50 °C at a rate of 10 °C/min and then reheated 220 °C at a rate of 10 °C/min. under N_2 flow rate of 100 mL/min. Mechanical strength such as modulus of elasticity and tensile strength was measured with a Zwick Universal Testing Machine (UTM) operating crosshead speed of 50 mm/min. For this test, the dumb-bell shape samples with the test size of 3.09 mm thickness and 3.2 mm width were prepared by using an injection molder at 190 °C. The test was conducted on four specimens for each sample and the average value was reported.

Results and discussion

Organically modified LDHs

The X-ray diffraction (XRD) patterns of LDHs modified with anionic surfactants (LA-LDH, PA-LDH, SA-LDH, DS-LDH, LP-LDH) are displayed in Fig. 1(A) together with the pristine Cl^- intercalated LDH (Cl-LDH). The XRD patterns of Cl-LDH showed well developed (*00l*) diffraction peaks corresponding to the basal spacing of 7.7 Å, indicating the formation of chloride intercalated Mg_2Al-LDH. After modifying LDH with anionic surfactants via coprecipitation or ion-exchange reaction, the

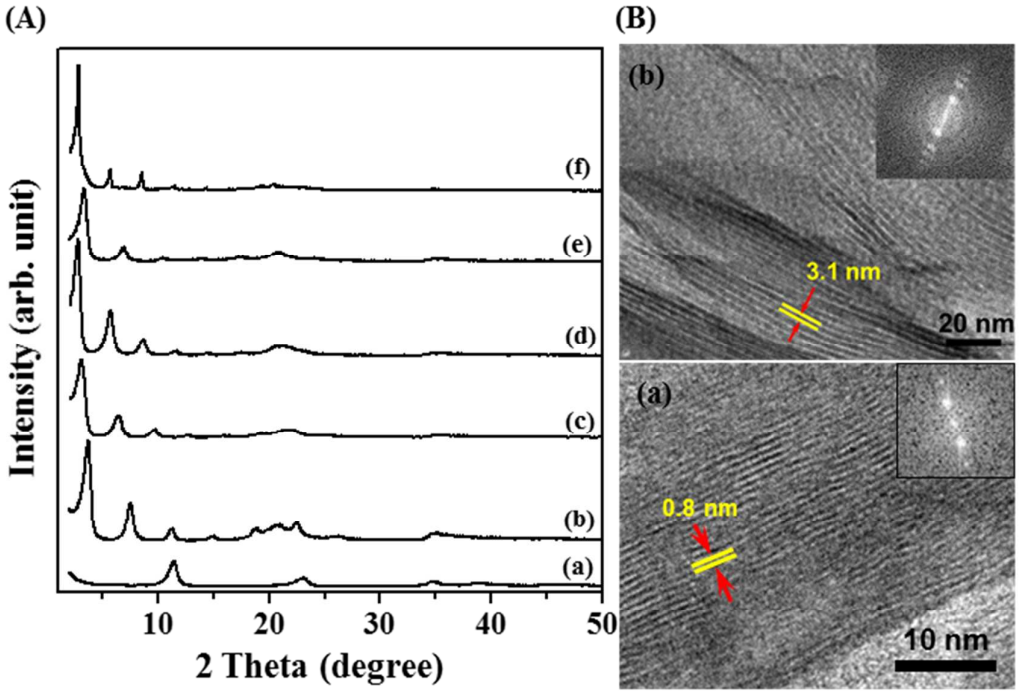

Fig. 1 (A) X-ray diffraction patterns (a) Cl-LDH, (b) LA-LDH, (c) PA-LDH, (d) SA-LDH, (e) DS-LDH and (f) LP-LDH, (B) TEM images and their corresponding FFT diffractograms (insets) of the cross-sectioned (a) Cl-LDH and (b) SA-LDH.

(*00l*) reflection peaks were shown to be well developed and shifted to the lower 2θ angle. The basal spacing of LA-, PA-, SA-, DS- and LP-LDH was determined to be 24.1 Å, 29.0 Å, 31.7 Å, 25.6 Å and 31.5 Å, respectively, which were in good agreement with the literature values of organo-LDHs within experimental error. [17-19] These increases of basal spacing compared to pristine Cl-LDH indicate the large anionic molecules were successfully intercalated into the LDH layers. Fig. 1(B) shows periodically ordered intercalation structure along the crystallographic c-axis to be confirmed by the cross-sectional TEM images and Fourier filtered images of Cl-LDH and SA-LDH. The basal spacing measured between the two lattice fringes for Cl-LDH and SA-LDH was determined to be 8 Å and 31 Å, respectively, which are in good agreement with those of determined from XRD measurements.

With the knowledge of the basal spacing, the layer thickness of LDH (4.8 Å) and the length of intercalated molecule, the interlayer structure of intercalated molecule can be suggested. In case of LA-, PA- and SA-LDH, the basal spacing of anionic surfactant modified LDH linearly increased with the number of carbon atoms in aliphatic carboxylic acid, suggesting a similar interlayer structure. For example, the molecular size of SA is estimated to be about 26.8 Å along the long axis based on the program, Chemdraw (version 8.0), and the thickness of LDH single sheet is 4.8 Å as shown in Fig. S2 (†ESI). And therefore, the basal spacing (31.7 Å) observed from XRD analysis is exactly the same as the sum of them (26.8 + 4.8 = 31.6 Å), indicating that SA molecules are oriented perpendicularly with monolayer structure inbetween LDH layers as shown in Fig. S2 (†ESI), not with tilted bilayer structure. Considering the layer charge distribution, the area demand of anionic surfactant molecule and the van der Waal's energy gain upon close packing of alkylchains in the layers, we strongly suggest the intracrystalline structure of organic surfactant molecules in LDH lattice as the interdigitated perpendicular monolayer structure with the d-spacing of 31.7 Å. The inter-gallery heights of LA-, PA- and DS-LDHs are similar to their organic molecular size, indicating that LA, PA and DS were also intercalated into the LDH with the perpendicular monolayer orientation with respect to the LDH layers. However, the basal spacing of LP-LDH (31.5 Å) is larger than the sum of the thickness of LDH (4.8 Å) and the molecular size of LP (21.5 Å), and smaller than the sum of the thickness of LDH layer and 2 times of the LP molecular size (perpendicular bi-layer). Therefore, it could be concluded that LP molecules were intercalated into LDH with the tilted bi-layer orientation, in which the expected tilting angle is 39°. The resulting organo-LDHs possess hydrophobic surface property due to long-chain aliphatic hydrocarbon of intercalated anionic surfactant covering the hydrophilic LDH surface.

Fourier transformed infrared spectra (FT-IR) of LDHs modified with anionic surfactants are shown in Fig. 2. A broad absorption peak between 3100 cm^{-1} and 3600 cm^{-1} is assigned to the O-H stretching vibration of the metal hydroxide layer and interlayer water. Due to the aliphatic alkyl chains in the used anionic surfactants, the strong absorption peaks at 2965 cm^{-1} and 2852 cm^{-1} correspond to the asymmetric and symmetric CH_2 stretching bands.[23,24] For LA-, PA- and SA-LDH,

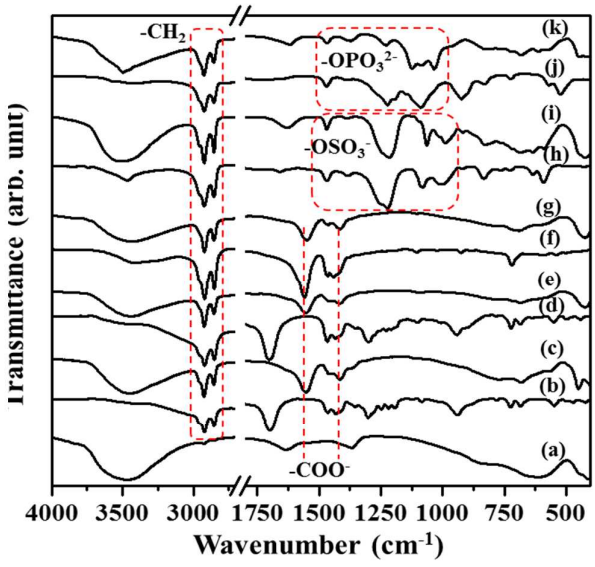

Fig. 2 FT-IR spectra of (a) Cl-LDH, (b) LA, (c) LA-LDH, (d) PA, (e) PA-LDH, (f) Na-SA, (g) SA-LDH, (h) DS, (i) DS-LDH, (j) LP and (k) LP-LDH.

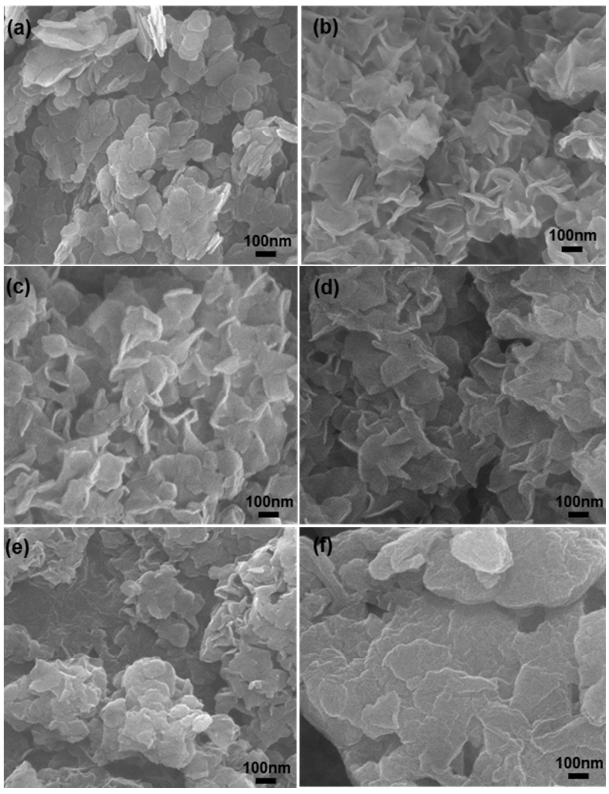

Fig. 3 Scanning microscopic images of (a) Cl-LDH (b) LA-LDH, (c) PA-LDH, (d) SA-LDH, (e) DS-LDH and (f) LP-LDH.

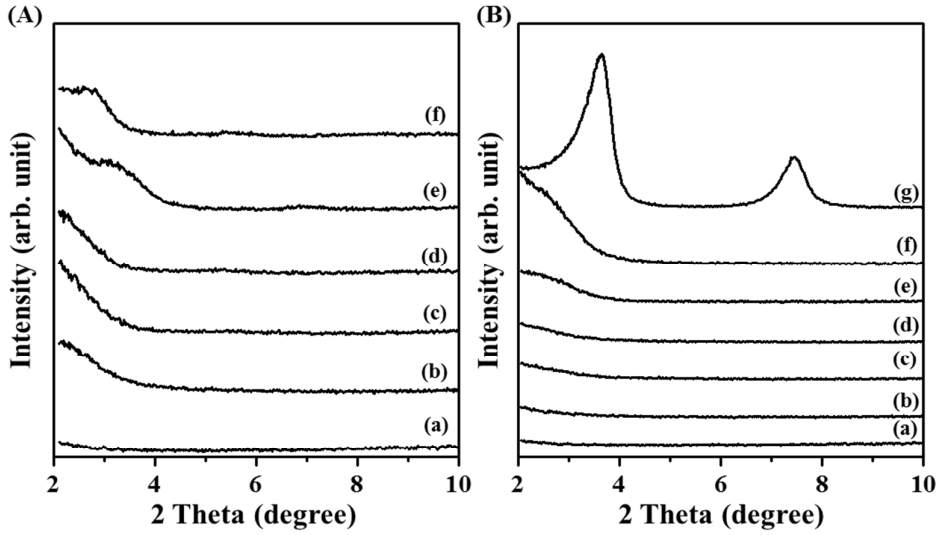

Fig. 4 XRD patterns of (A) (a) pristine PP, (b) 3 phr LA-LDH/PP, (c) 3 phr PA-LDH/PP, (d) 3 phr SA-LDH/PP, (e) 3 phr DS-LDH/PP and (f) 3 phr LP-LDH/PP, and (B) (a) pristine PP, (b) 1 phr LA-LDH/PP, (c) 3 phr LA-LDH/PP, (d) 6 phr LA-LDH/PP, (e) 9 phr LA-LDH/PP, (f) 12 phr LA-LDH/PP and (g) LA-LDH, respectively.

two peaks at 1550 cm^{-1} and 1414 cm^{-1}, assigned to the asymmetric and symmetric stretching bands of carboxylate anion, indicate that all the carboxylic acid groups in LA, PA and SA were completely deprotonated and have an electrostatic interaction with cationic LDH layers.[23-24] In DS-LDH, the peaks corresponding to the asymmetric and symmetric stretching vibration of sulfate group were observed at 1224 cm^{-1} and 1074 cm^{-1}.[18,24] For LP-LDH, the vibration bands of phosphate anion are observed at 1229 cm^{-1}, 1126 cm^{-1} and 1087 cm^{-1}.[24,25] The peaks between 400 cm^{-1} and 700 cm^{-1} were assigned to the vibration bands of M-O-M in the brucite-like metal hydroxide layer.[18] All the modified LDHs showed characteristic vibration bands of anionic functional group of each surfactant, indicating electrostatic interaction with cationic LDH layers.

The morphology and particle size of organo-LDHs were characterized by SEM analysis (†ESI Table S1, Fig. 3). As can be seen in Figure 3, Cl-LDH and all the organo-LDHs have the aggregated plate-like morphology. The ab plane size of primary particles was evaluated to be 100 nm - 300 nm, and the average particle sizes for Cl-LDH and the organo-LDHs were in the range of 175 nm ~ 244 nm. Thicknesses were less than 20 nm, except LP-LDH which had a strongly aggregated morphology attributed to strong electrostatic interaction between LDH layers and divalent LP anions.

Organo-LDH/PP nanocomposites

The hydrophobically modified LDHs were well-dispersed in organic solvents such as xylene (†ESI Fig. S1). The hydrophobically modified LDH promotes the intercalation of PP into the interlayers of LDH due to the increased compatibility and decreased electrostatic interaction between LDH layers. XRD patterns of PP nanocomposites containing 3 phr organo-LDH are displayed in Fig. 4(A) together with pristine PP. The sharp and well developed (*00l*) peaks of LA-, PA- and SA-LDH shown in Fig. 1 disappeared after the formation of nanocomposite with PP via solution-blending method. The well stacked layers of the organically modified LDHs along the c-axis were exfoliated and dispersed in PP matrix. However, for the nanocomposites (DS-, LP-LDH/PP), the (*00l*) peak intensity and shape of DS- and LP-LDH became weaker, broader, and slightly shifted to lower 2θ angle, indicating that a part of organo-LDH layers were incompletely exfoliated, and dispersed in PP matrix. Such a difference in exfoliation of organo-LDHs in PP would be surely due to the fact that a difference in bond strength between anionic functional group of organic surfactant and the positively charged LDH layers. In other words, the LDH layer modified with alkylcarboxylate was found to be better exfoliated in xylene and well-dispersed in PP matrix than LDH layer modified with alkylsulfate and alkylphosphate. This phenomenon could be explained by the net charge and the size of anionic head group of anionic surfactant. Since LP is a divalent anion, the density of hydrophobic lauryl group adsorbed on the hydrophilic LDH surface of LP-LDH would be less than LA-LDH, indicating that the surface of LP-LDH. Consequently the surface of LP-LDH is less hydrophobic than LA-LDH. Anionic functional groups, such as phosphate and sulfate, are more polar and larger than carboxylate functional groups. Therefore, LP-LDH and DS-LDH are less hydrophobic compared to LA-, PA- and SA-LDH, resulting in partially exfoliated LP-LDH and DS-LDH and less homogeneous dispersion of LDH layers in PP matrix.

Furthermore, the changes of the dispersion degree of organo-LDH in PP matrix as a function of the loading content of LA-LDH were investigated. XRD patterns of 1 phr - 12 phr LA-LDH/PP nanocomposites are displayed in Fig. 4 (B). When LA-

LDH was loaded up to 9 phr, (*00l)* diffraction peaks of LA-LDH were invisible, but at 12 phr, broad peaks shifted to lower 2θ angle could be observed, indicating the presence of partially intercalated LA-LDH. Based on these results, the maximum loading content of LA-LDH was determined to be 9 phr in order to synthesize nanocomposites that were exfoliated and well-dispersed LA-LDH in PP matrix.

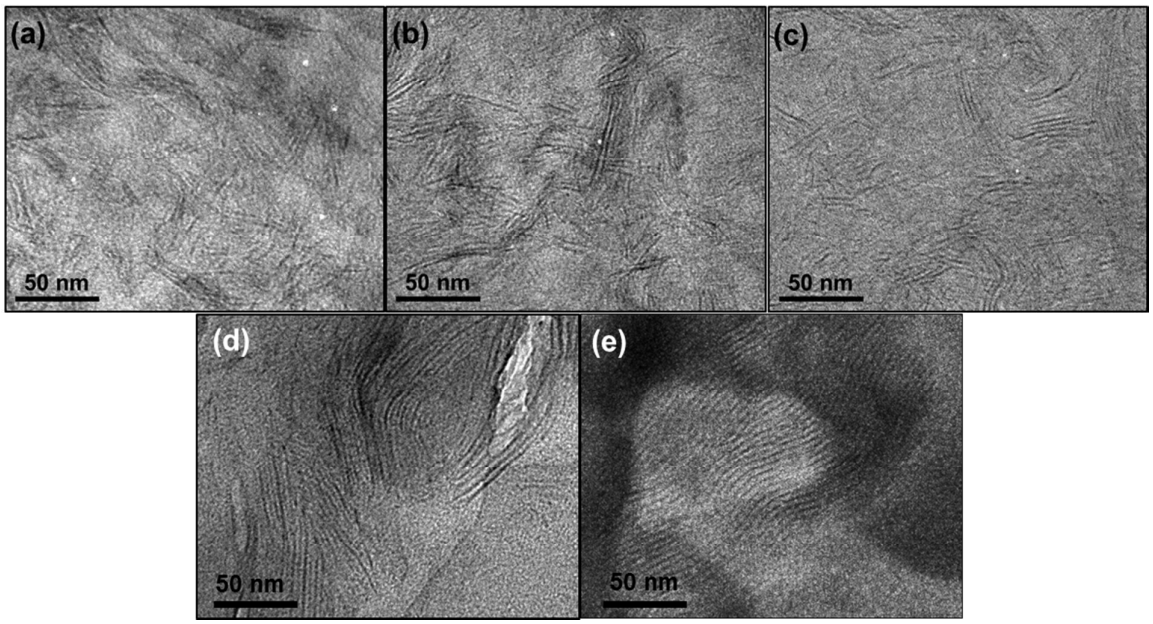

Fig. 5 Transmission electron microscopic images of (a) 3 phr LA-LDH/PP (b) 3 phr PA-LDH/PP (c) 3 phr SA-LDH/PP, (d) 3phr DS-LDH/PP and (e) 3phr LP-LDH/PP, respectively.

In order to confirm the dispersion degree of LA-, PA-, SA- , DS- and LP-LDH in PP matrix, the cross-sectioned morphologies of those nanocomposites were measured by TEM. As in Fig. 5, most layers of LDH modified with LA and PA were sufficiently separated from each other, and randomly dispersed in PP matrix, indicating that most LDH layers were exfoliated in PP matrix. However, within SA-LDH/PP nanocomposite, swelled LDH structure with several layers (3 - 6 layers) and sufficiently separated layers were observed, indicating that both the PP intercalated LDH layers and the exfoliated LDH layers existed

concurrently. Since the hydrophobic van der Waals interaction of closely packed SA molecules in LDH inter-gallery is stronger than those of LA and PA, it is difficult to obtain PP nanocomposite with completely exfoliated SA-LDH layers. As shown in Figure 5 (d) and (e), however, one can see clearly that DS-LDH and LP-LDH particles still remained mostly their multi-stacked lamellar structure even after the solution blended in PP matrix, while LA-LDH, PA-LDH and SA-LDH ones were exfoliated and well dispersed in PP matrix [Figure 5 (a)~(c)], which is in good agreement with the result obtained from low-angle XRD analysis [Figure 4(A)].

Fig. 6 represents the wide angle XRD patterns and differential thermal analysis (DTA) cooling scan thermograms of PP and organo-LDH/PP nanocomposites. All the XRD patterns of organo-LDH/PP nanocomposites were apparently similar to that of pristine PP (monoclinic α form),[27] indicating that the crystal structure of PP matrix was unchanged after the nanocomposition with organo-LDH. And the degree of crystallinity[26,27] of PP could be calculated by using Fullprof program[28] and summarized in Table S2 (†ESI). After the formation of PP nanocomposites with organo-LDH, the degree of crystallinity of intact PP (48 %) was compared to that of PP nanocomposites, which was negligibly decreased to 43~47 % for those with well dispersed organo-LDH such as LA-LDH, PA-LDH and SA-LDH, but retained to around 48% and 50% for those with in-homogeneously dispersed DS-LDH and LP-LDH, respectively, which seemed to be the same as that of intact PP within the experimental error. Furthermore, the intensity ratio of the (040) peak at 16.8° to the (110) peak at 14.0° of PP increased after nanocomposition with organo-LDH, indicating the PP crystallized with the organo-LDH nanosheet direction to some degree. The melting point of all PP nanocomposites was similar to pristine PP (165 ± 1 °C) based on the DTA analysis (†ESI Fig. S3). However, the DTA cooling scanning curves showed that the exothermic peak position of PP attributed to the recrystallization of PP was shifted to a high temperature from 114.2 °C to 118 °C after nanocomposition with 3 phr organo-LDH. With the increase of loading content of LA-LDH up to 6 phr, the cold crystallization temperature slightly increased up to 119.6 °C, while the further loading content of LA-LDH reduced the cold crystallization temperature to 117.9 °C (at 12 phr). This increase of cold crystallization temperature indicates the organo-LDH layers playing a role of efficient nucleating agents for the crystallization of PP matrix like the silicate layers in clay/PP nanocomposites.[29]

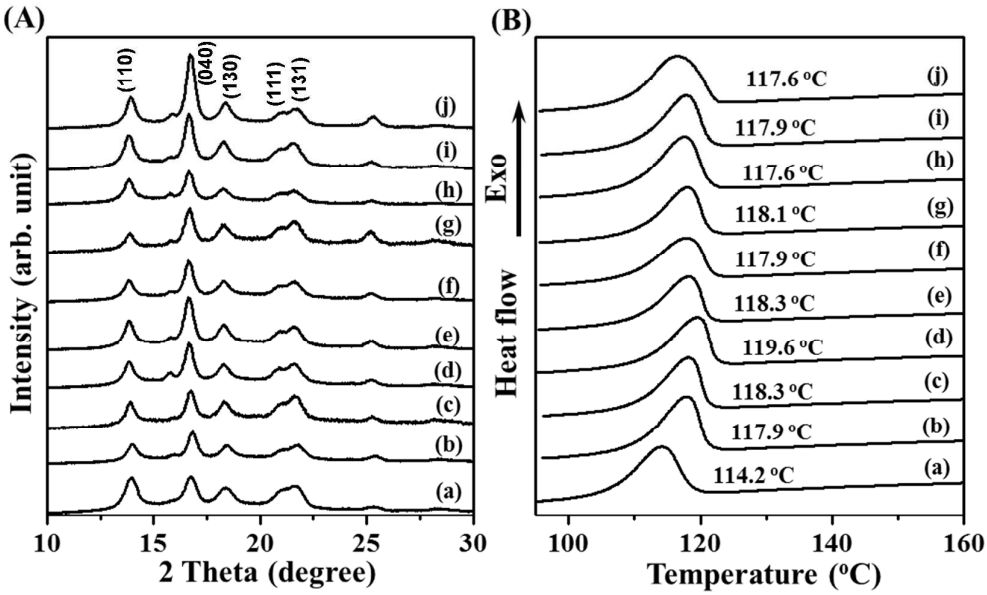

Fig. 6 (A) XRD patterns and (B) cooling scanning DTA curves of (a) pristine PP, (b) 1 phr LA-LDH/PP, (c) 3 phr LA-LDH/PP, (d) 6 phr LA-LDH/PP, (e) 9 phr LA-LDH/PP, (f) 12 phr LA-LDH/PP, (g) 3 phr PA-LDH/PP, (h) 3 phr SA-LDH/PP, (i) 3 phr DS-LDH/PP and (j) 3 phr LP-LDH/PP.

The thermal stability of PP nanocomposites depending on the kind of organo-LDHs and the loading content were evaluated with TGA under air atmosphere with 200 mL/min low rate. TGA curves of organo-LDH/PP nanocomposites depending on the organic modifier of LDH are displayed in Fig. 7(a) together with pristine PP. The major weight loss of the pristine PP by the thermal decomposition appeared at 273 °C to 373 °C. However, the thermal decomposition temperature of PP containing organically modified LDH significantly shifted to higher temperatures compared to pristine PP, which was also observed in other nano-filler/polymer composites.[7,19,30] The thermal stability of organo-LDH/PP nanocomposites is summarized in Table 1 and Table S3 (†ESI) based on 50% weight loss temperature ($T_{0.5}$). $T_{0.5}$ of 3 phr LA-LDH/PP nanocomposite was 383 °C, which is higher than pristine PP (334 °C) by 49 K, which is comparable to the PP nanocomposite with distearyldimethylammonium intercalated montmorillonite (DSDMA-MMT, $\Delta T_{0.5}$ = 48K) even though the content of LA-LDH in PP (~3%) is less than that of DSDMA-MMT in PP (5%).[31] $T_{0.5}$ of 3 phr PA- and SA-LDH/PP nanocomposites increased to 391 °C, indicating improvement of the thermal stability by 57 K compared to pristine PP. This improvement of thermal stability is comparable to PP/LDH prepared with nanosized LDH.[18] $T_{0.5}$ of 3 phr LP- and DS-LDH/PP also increased to 371 °C and 372 °C. This enhanced thermal stability is attributed to the homogeneous dispersion of the LDHs nanoplates in PP matrix with very high interfacial contact area, the suppression of heat transfer in the polymer by the dispersed nanoplates, and the endothermic reaction of LDH by dehydroxylation.[18,30] The thermal stability of LA-, PA- and SA-LDH/PP nanocomposites is higher than LP- and DS-LDH/PP nanocomposites since LA-, PA- and SA-LDH were exfoliated and well-dispersed in PP matrix. Yet, part of LP- and DS-LDHs were aggregated and dispersed in PP matrix as shown in XRD analysis (Fig. 4). The thermal stability of PP nanocomposites, depending on the loading content of LA-LDH, was also investigated. TGA curves are displayed in Fig. 7(b) together with pristine PP. Even 1 phr loading of LA-LDH in PP matrix gave rise to a significant increase in $T_{0.5}$ from 334 °C to 377 °C ($\Delta T_{0.5}$ = 43 K), which is higher than $\Delta T_{0.5}$ for 1% CNT loaded PP (30 K).[32] Increasing the loading content of LA-LDH from 1 phr to 12 phr gradually increased $T_{0.5}$ from 377 °C (1 phr) to 395 °C (12 phr), attributed to the increase of endothermic reaction energy by the dehydroxylation of LDH with the increase of loading content of LA-LDH in PP matrix,

Table 1. Thermal stability of various PP nanocomposites.

Samples	Organo-LDH content (phr)	$T_{0.5}$ (°C)[a]	$\Delta T_{0.5}$ (K)[b]
PP	0	334	-
LA-LDH/PP	1	377	43
LA-LDH/PP	3	383	49
LA-LDH/PP	6	386	52
LA-LDH/PP	9	389	55
LA-LDH/PP	12	395	61
PA-LDH/PP	3	391	57
SA-LDH/PP	3	391	57
DS-LDH/PP	3	371	37
LP-LDH/PP	3	373	39

[a] $T_{0.5}$ is the temperature at 50% weight loss,
[b] $\Delta T_{0.5} = T_{0.5} - \Delta T_{0.5(\text{pristine PP})}$.

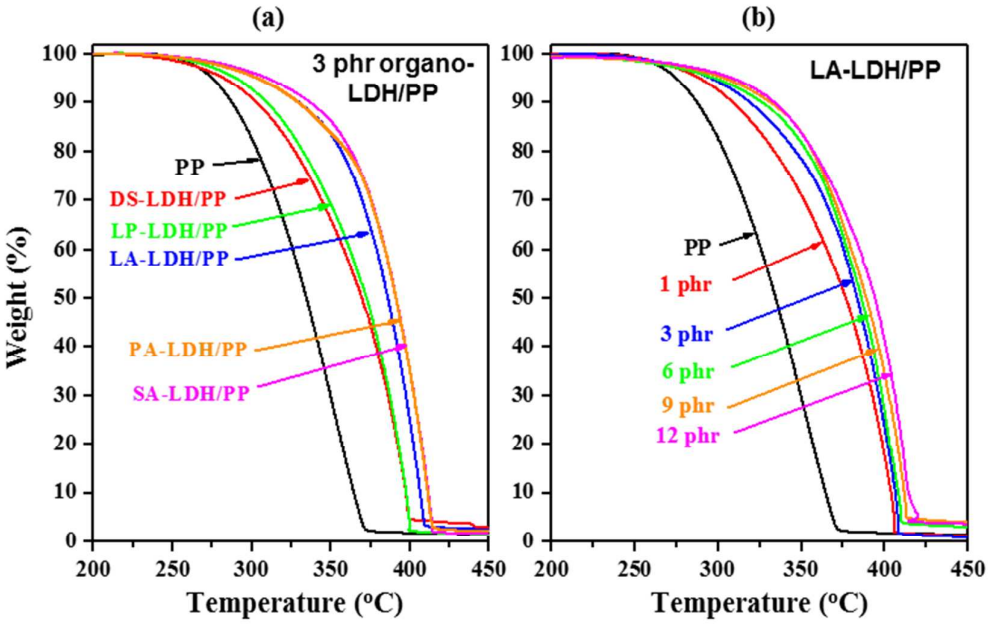

Fig. 7 TG curves of PP and organo-LDH/PP nanocomposites depending on (a) the kind of organo-LDHs and (b) the loading content of LA-LDH.

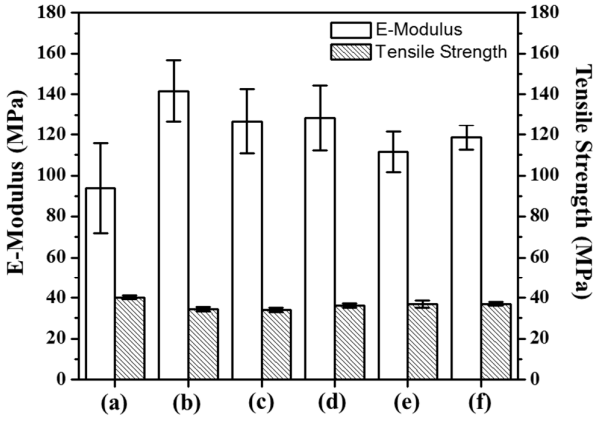

Fig. 8 Elastic modulus and tensile strength of (a) PP, (b) 3 phr LA-LDH/PP, (c) 3 phr PA-LDH/PP (d) 3 phr SA-LDH/PP (e) 3 phr DS-LDH/PP and (f) 3 phr LP-LDH/PP.

indicating that LDH nanosheet could play a role of flame retardant materials.

Fig. 8 shows the elastic modulus and the tensile strength of PP nanocomposites containing organo-LDH depending on the type of anionic surfactant. Generally, mechanical properties were affected by the dispersion of inorganic filler in PP matrix. As in Figure 8, LA-, PA-, SA-LDH/PP nanocomposites show significantly increased elastic modulus compared to pristine PP, while LP- and DS-LDH/PP nanocomposites were only slightly improved. This result is strongly related with the exfoliation degree as shown in XRD and TEM results of organo-LDH/PP nanocomposites. Highly exfoliated LDH layers dispersed in PP matrix, such as LA-, PA- and SA-LDH, give rise to larger interfacial contact area with polymer due to the higher aspect ratio of LDH nanosheets. The increased elastic modulus is attributed to the improvement of stiffness of PP by adding exfoliated LDHs.[33] However, organo-LDHs did not contribute to the increase in tensile strength, possibly caused by the weak adhesion property between organo-LDH and PP matrix, which was also observed in the poly(trimethylene terephthalate)/clay nanocomposites.[34]

Conclusions

Hydrophobic modification of hydrophilic LDH layers were performed effectively by incorporating series of anionic surfactants within LDH galleries. The PP nanocomposites containing highly dispersed LDH layers were successfully prepared via solvent-blending method by using the hydrophobically-modified LDHs. The dispersion degree of organically modified LDHs within PP matrix was affected by the type of organic modifiers. LA-, PA- and SA-LDH with carboxylate anionic group were exfoliated and well dispersed in PP matrix, while DS- and LP-LDH with sulfate and phosphate anionic group were partially exfoliated and dispersed in PP matrix. The thermal stability of all the organo-LDH/PP nanocomposites was significantly improved. Even 1 phr loading of LA-LDH improved the thermal stability of PP by 43 ^{o}C in $T_{0.5}$ with gradual further increases upto 61 ^{o}C at 12 phr. Thermal stabilities of 3 phr LA-LDH/PP, PA-LDH/PP and SA-LDH/PP was higher than those of 3 phr DS-LDH/PP and LP-LDH/PP. These would have been related with the better dispersibility of LA-, PA- and SA-LDH in PP matrix, originated from the hydrophobicity and the size of anionic functional moieties. The elastic modulus of 3 phr LA-LDH/PP were improved by approximately 50% compared to that of pristine PP due to the well dispersed nature of organo-LDH nanosheets in PP matrix, while the tensile strength did not decrease substantially within the added contents of organo LDH. The thermal stability and the mechanical property of organo-LDH/PP nanocomposites were affected by the hydrophobicity of organo-LDH layers. These results suggest that it is very important to select a suitable anionic surfactant to modify the surface of LDH properly depending upon the desired functions of polymer materials like high thermal stability and mechanical strength. All the present results would be beneficial not only polymer scientists, but also all composite material researchers.

Acknowledgements

This work was supported by grants from the Ministry of Knowledge Economy (1004 1239) and the National Research Foundation of Korea (NRF) grant funded by the Korea government (MSIP) (2005-0049412).

Notes and references

1 D. H.Park, S. J. Hwang, J. M. Oh, J. H. Yang and J. H. Choy, *Prog. Polymer Sci.,* 2013, **38**, 1442-1486.
2 D. H. Kim, P. D. Fasulo, W. R. Rodgers and D. R. Paul, *Polymer* 2007, **48**, 5308-5323.
3 W. Gianelli,; G. Ferrara, G. Camino, G. Pellegatti, J. Rosenthal and R. C. Trombini, *Polymer* 2005, **46**, 7037-.7046.
4 R. Krishnamoorti and R. A. Vaia *Chem. Mater.*, 1996, **8**, 1728-1734
5 R. A. Vaia and E. P. Giannelis, *MRS Bull*. 2001, **26**, 394-401.
6 (a) T. McNally and P. Pötschke*., Polymer-Carbon Nanotube Composites - Preparation, Properties and Applications*, Woodhead Publishing, Cambridge (U.K.), 2011; (b) T. Kashiwagi, F. Du, J. F. Douglas, K. I. Winey, R. Harris Jr..and J. R. Shields, *Nat. Mater.*, 2005, **4**, 928-933.
7 M. Moniruzzaman and K. I. Winey, *Macromolecules*, 2006, **39**, 5194-5205.
8 B. M. Novak, *Adv. Mater*., 1993, **5**, 422-433.
9 G. Li, L. Wang, H. Ni and C. U. Pittman Jr., *J. Inorg. Organomet. Polym.* 2001, **11**, 123-154.
10 Y. Kojima, A. Usuki, M. Kawasumi, A. Okada, Y. Fukushima, T. Kurauchi and O. Kamigaito, *J. Mater. Res.*, 1993, **8**, 1185-1189.
11 Q. Wang and D. O'Hare, *Chem. Rev*. 2012, **112**, 4124-4155.
12 Z. Lu, W. Xu, W. Zhu, Q. Yang, X. Lei, J. Liu, Y. Li, X. Sun and X. Duan, *Chem. Commun.,* 2014, **50**, 6479-6482.
13 S. Miyata and M. Kuroda, *US Patent 4,299,759***, 1981,** to Kyowa Chem. Ind. Ltd.

14 (a) K. M. Kim, C. B. Park, A. J. Choi, J. H. Choy and J. M. Oh, *Bull. Korean Chem. Soc.*, 2011, **32**, 2217-2221; (b) Q. Wang, J. Luo, Z. Zhong and A. Borgna, *Energy Environ. Sci*. **2011**, *4*, 42-55.

15 (a) J. H. Choy, S. Y. Kwak, J. S. Park, Y. J. Jeong and J. Portier, *J. Am. Chem. Soc.* 1999, **121***,* 1399-1400; (b) G. Choi, O. J. Kwon, Y. Oh, C. O. Yun and J. H. Choy, J. H. *Scientific Reports*, 2014, **4**, 4430, doi:10.1038/srep04430; (c) M. H. Kim, D. H. Park, J. H. Yang, Y. B. Choy and J. H. Choy, *Int. J. Pharmaceut,* 2013, **444**, 120-127.

16 Y. J. Lin and D. Q. Li, *Polym. Degrad. Stab.*, 2005, **88**, 286–293.

17 (a) T. Y. Tsai, B. Naveen, W. C. Shiu and S. W. Lu, *RSC Adv.*, 2014, **4**, 25683- 25691; (b) J. Gaume, S. Therias, F. Leroux, A. Rivaton and J. L. Gardette, *J. Appl. Polym. Sci.* 2013, **129**, 1345-1349.

18 Q. Wang, X. Zhang, C. J. Wang, J. H. Zhu, Z. H. Guo and D. O'Hare, D. *J. Mater. Chem.*, **2012**, *22*, 19113-19121.

19 C. Manzi-Nshuti, P. Songtipy, E. Manias, M. M. Jimenez-Gasco, J. M. Hossenlopp and C. A. Wilkie, *Polymer*, 2009, **50**, 3564–3574.

20 P. J. Purohit, J. E. Huacuja-Sánchez, D. Y. Wang, F. Emmerling, A. Thünemann, G. Heinrich and A. Schönhals, *Macromolecules,* 2011, **44**, 4342–4354.

21 W. Gao, J. Wu, Q.Wang, C. A. Wilkie and D. O'Hare, *J. Mater. Chem. A*, 2014, **2**, 10996-11016.

22 The "phr' means the parts per hundred rubber (polymer), as well known in polymer community. In this manuscript, "phr" is the g weight of added organo-LDH per 100 g of PP.

23 J. H. Choy, Y. M. Kwon, K. S. Han, S. W. Song and S. H. Chang, *Mater. Lett.* 1998, **34**, 356-363.

24 D. L. Pavia, G. M. Lampman and G. S. Kriz, *Introduction To Spectroscopy 2nd ed.*, Harcourt Brace College Publishers, Fort Worth, 1996.

25 F. R. Costa, A. Leuteritz, U. Wagenknecht, D. Jehnichen, L. Haussler and G. Heinrich, *Appl. Clay Sci.*, 2008, **38**, 153-164.

26 L. S. Zevin and G. Kimmel, *Quantitative X-ray Diffractormetry*, Springer-Verlag, New York, 1995.

27 M. F. S. Lima, M. A. Z. Vasconcello and D. Samios, *J. Polym. Sci. Pt.B-Polym. Phys.*, 2002, **40**, 896-903.

28 J. Rodriguez-Carvajal, *Fullprof 2000: A Rietveld Refinement and Pattern Matching Analysis Program*, April 2008, Laboratoire Léon Brillouin (CEA-CNRS).

29 X. Liu and Q. Wu, *Polymer,* 2001, **42**, 10013-10019.

30 K. T. Gilman and T. Kashiwagi, T. *Polymer-Clay Nanocomposites*, ed. T. J. Pinnavaia and G. W. Beall, , John Wiley & Sons, New York. 2000.

31 H. Qin, S. Zhang, C. Zhao, M. Feng, M. Yang, Z. Shu and S. Yang, *Polym. Degrad. Stabil.* 2004, **85**, 807-813.

32 M. V. Jose, D. Dean, J. Tyner, G. Price and E. Nyairo, *J. Appl. Polym. Sci.* 2007, **103**, 3844-3850.

33 M. Modesti, A. Lorenzetti, D. Bon and S. Besco, *Polymer*, 2005, **46**, 10237-10245.

34 K. Y.Wang, Y. M. Chen and Y. Zhang, *Polymer*, 2008, **49**, 3301-3309.

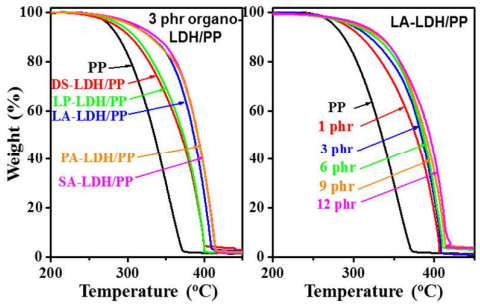

The thermal stability of PP was significantly improved after the formation of PP nanocomposition with organo-LDH, which was affected by the type of organic modifier in organo-LDH and the loading amount of organo-LDH.